Druse clinopyroxene in D'Orbigny angritic meteorite studied by single-crystal X-ray diffraction, electron microprobe analysis, and Mössbauer spectroscopy

Yassir A. ABDU[1]*, Rosa B. SCORZELLI[2], Maria E. VARELA[3], Gero KURAT[4], Izabel de Souza AZEVEDO[2], Silvana J. STEWART[5], and Frank C. HAWTHORNE[1]

[1]Department of Geological Sciences, University of Manitoba, Winnipeg, Manitoba R3T 2N2, Canada
[2]Centro Brasileiro de Pesquisas Físicas, Rua Xavier Sigaud 150, 22290-180 Rio de Janeiro, Brazil
[3]Complejo Astronómico El Leoncito (CASLEO), Av. España 1512 Sur, CP J5402DSP, San Juan, Argentina
[4]Naturhistorisches Museum, Burgring 7, 1010 Vienna, Austria
[5]IFLP, CONICET, Depto. De Física, Facultad de Cs. Exactas, Universidad Nacional de La Plata, Argentina
*Corresponding author. E-mail: abdu@cc.umanitoba.ca

Abstract–The crystal structure of druse clinopyroxene from the D'Orbigny angrite, $(Ca_{0.944} Fe^{2+}_{0.042} Mg_{0.010}Mn_{0.004})$ $(Mg_{0.469}Fe^{2+}_{0.317}Fe^{3+}_{0.035}Al_{0.125}Cr_{0.010}Ti_{0.044})$ $(Si_{1.742}Al_{0.258})$ O_6, $a = 9.7684(2)$, $b = 8.9124(2)$, $c = 5.2859(1)$ Å, $\beta = 105.903(1)°$, $V = 442.58$ Å^3, space group $C2/c$, $Z = 2$, has been refined to an R_1 index of 1.92% using single-crystal X-ray diffraction data. The unit formula, calculated from electron microprobe analysis, and the refined site scattering values were used to assign site populations. The distribution of Fe^{2+} and Mg over the M1 and M2 sites suggests a closure temperature of 1000 °C. Mössbauer spectroscopy measurements were done at room temperature on a single crystal and a powdered sample. The spectra are adequately fit by a Voigt-based quadrupole-splitting distribution model having two generalized sites, one for Fe^{2+} with two Gaussian components and one for Fe^{3+} with one Gaussian component. The two ferrous components are assigned to Fe^{2+} at the M1 site, and arise from two different next-nearest-neighbor configurations of Ca and Fe cations at the M2 site: (3Ca,0Fe) and (2Ca,1Fe). The Fe^{3+}/Fe_{tot} ratio determined by Mössbauer spectroscopy is in agreement with that calculated from the electron microprobe analysis. The results are discussed in connection with the redox and thermal history of D'Orbigny.

INTRODUCTION

D'Orbigny is an angrite meteorite found in the Buenos Aires province of Argentina in 1979. Its richness in glasses, the abundance of hollow shells, and the presence of abundant open druses make it a special member of the angrites (Varela et al. 2003). Angrites, a small and rare group of achondrites, are generally believed to be products of igneous processes on a differentiated parent body (Mittlefehldt et al. 2002; Floss et al. 2003). However, recent detailed studies of D'Orbigny have shown that it has a very complex history, and a non-igneous origin from refractory solar nebula condensates of a chondritic character has been suggested (Kurat et al. 2004; Varela et al. 2005).

The major minerals in D'Orbigny are olivine, anorthite, and clinopyroxene. The clinopyroxene is present both in the groundmass and in open druses, and was described as augite (Kurat et al. 2004). The current pyroxene nomenclature (Morimoto 1989) classifies both groundmass and druse

pyroxenes from D'Orbigny not as augite (which has Ca < 0.90 apfu), but as diopside-hedenbergites with various adjectival modifiers. The groundmass pyroxene is compositionally zoned, whereas the druse pyroxene is homogeneous and has a composition very similar to that of the cores of the groundmass pyroxene (Kurat et al. 2004). The average core composition is given as $En_{27}Fs_{22}Wo_{51}$. Recalculation of the analyses given by Kurat et al. (2004) indicate the presence of significant amounts of tetrahedrally coordinated Al and octahedrally coordinated Al, Cr^{3+} and Ti, and expression of the composition of the pyroxene in terms of En, Fs, and Wo components ignores these additional constituents. We consider this issue more fully in the Appendix. The average composition of the core groundmass pyroxene is $Di_{0.50}Hd_{0.27}En_{0.00}Fs_{0.06}$ $CaTs_{0.14}$ $TiCaTs_{0.03}$ $(Di_{0.494}$: aluminian ferroan titanoan diopside), the rim groundmass pyroxene is $Di_{0.00}Hd_{0.83}En_{0.00}Fs_{0.02}$ $CaTs_{0.00}$ $TiCaTs_{0.13}$ $(+TiHd_{0.02})$ (subsilicic aluminian titanian hedenbergite), and the druse pyroxene is

$Di_{0.48}Hd_{0.25}En_{0.00}Fs_{0.06}$ $CaTs_{0.17}$ $TiCaTs_{0.04}$ (aluminian ferroan titanoan diopside) (Appendix).

Calcium pyroxenes along or near the join diopside $(CaMgSi_2O_6)$-hedenbergite $(CaFe^{2+}Si_2O_6)$ are monoclinic with the space group *C2/c*. The larger and more distorted M2 polyhedron is usually occupied by Ca and Na, whereas the M1 polyhedron contains Mg, Fe^{2+}, trivalent and tetravalent cations (Cameron and Papike 1980). The intracrystalline Fe^{2+}-Mg distribution between the M1 and M2 sites is very useful in tracing the thermal history of the host rock (McCallister et al. 1976; Molin and Zanazzi 1991; Malgarotto et al. 1993). The distribution coefficient, K_D, is defined as:

$$K_D = Fe^{2+}(M1).Mg(M2)/Fe^{2+}(M2).Mg(M1)$$

Mössbauer spectroscopy is a very valuable technique in determining Fe^{3+}/Fe^{2+} ratio and Fe site occupancy in Fe-containing minerals. It has been used effectively in obtaining site populations in orthopyroxenes using the relative areas of the M1 and M2 doublets (Dundon and Hafner 1971; Skogby et al. 1992). However, in Ca-rich clinopyroxenes, it is very difficult to obtain accurate Fe site distributions due to problems such as exsolution intergrowths and next-nearest-neighbor (NNN) effects of Ca atoms at the M2 site (Williams et al. 1971; Dowty and Lindsley 1973).

Here we characterize D'Orbigny druse clinopyroxene using single-crystal X-ray diffraction, electron-microprobe analysis, and Mössbauer spectroscopy in order to determine the Fe^{2+}-Mg distribution between the M1 and M2 sites and the oxidation state of Fe. This study was undertaken to create a state-of-the-art crystallographic analysis of this unusual pyroxene, which should help to quantify some of the parameters related to the thermal history of this rock. We also hope to gain an improved understanding of the genesis of angrites.

EXPERIMENTAL

A druse clinopyroxene crystal ($\sim400 \times 150 \times 80$ µm) was cut into two equal pieces; one was used for single-crystal X-ray diffraction (Xl.1) and the other for Mössbauer spectroscopy (Xl.2).

The Xl.1 crystal ($\sim200 \times 150 \times 80$ µm), which is inclusion-free and shows sharp extinction under a polarizing microscope, was attached to a glass fiber and mounted on a BRUKER P4 four-circle diffractometer equipped with monochromatic Mo$K\alpha$ radiation and a 4K CCD area detector. X-ray diffraction intensities were collected up to 60° 2θ and unit-cell parameters (Table 1) were refined using least squares. An absorption correction was done using the Bruker program SADABS.

The crystal used for collection of the X-ray intensity data was subsequently mounted in epoxy, polished, and analyzed

with a CAMECA SX-100 electron microprobe operating in wavelength-dispersion mode with the following conditions: excitation voltage: 15 keV; specimen current: 20 nA; beam size: 5 µm; peak count time: 20 s; background count time: 20 s. The crystal was analyzed at ten points, and the mean chemical composition is given in Table 4, together with the unit formula normalized to six oxygen atoms.

Transmission Mössbauer spectroscopy measurements were done at room temperature (RT) on the single crystal Xl.2 and on a powdered sample using a $^{57}Co(Rh)$ point source. For preparing the powdered Mössbauer absorber, ~1 mg of sample was mixed with sugar and finely ground under acetone to avoid oxidation. The mixture was then loaded into a Pb ring (2 mm inner diameter) and covered by tape on both sides. The resultant Mössbauer absorber contains ~3 mg Fe/cm^2. The spectra were analyzed using a Voigt-based quadrupole-splitting-distribution (QSD) method (Rancourt and Ping 1991). The center shift (CS) is given relative to α-Fe at room temperature.

RESULTS AND DISCUSSION

Structure Refinement and Site Populations

The crystal structure was refined to an R1 index of 1.92% using the SHELXTL Version 5.1 software (Sheldrick 1997) with anisotropic-displacement parameters for all sites. Scattering curves for neutral atoms were taken from the *International tables for X-ray crystallography* (Ibers and Hamilton 1992), and site-occupancies were refined at the M1 (Mg + Fe) and M2 (Ca) sites. Difference-Fourier synthesis showed a residual electron-density peak at 0.65 Å from the M2 site along the y-axis, corresponding to the M2′ site (Bruno et al. 1982); the occupancy of this site was refined as Fe. Final atom coordinates and equivalent isotropic-displacement parameters are listed in Table 2. Selected interatomic distances and angles are given in Table 3.

The T Site

As Si and Al have very similar scattering factors for X-rays, the site occupancies cannot be refined directly from diffraction data and the <T–O> distance must be taken into account for assigning site populations. The calculated <T–O> distance of 1.649 Å (using the equation of Hazen and Finger (1977): <T–O> = 1.634 + 0.117 × $^{IV}Al/(^{IV}Al+Si)$, where ^{IV}Al and Si are taken from the unit formula in Table 4) is in excellent agreement with the observed <T–O> distance of 1.650 Å. Therefore, 0.258 Al and 1.742 Si (*apfu*) were assigned to the T-site (Table 5).

The M(1,2) Sites

The total refined scattering at the M1,2 sites (37.6 *epfu*) is in very close agreement with the total effective scattering of the M1,2 cations obtained from EMPA (37.8 *epfu*), Table 1. This allows the use of the unit formula (Table 4) as a guide for

Table 1. Crystallographic data and structure refinement information for D'Orbigny druse clinopyroxene.

a (Å)	9.7684(2)	Crystal size (μm)	$200 \times 150 \times 80$
b (Å)	8.9124(2)	Radiation/ filter	Mo$K\alpha$/graphite
c (Å)	5.2859(1)	Unique reflections	649
β (°)	105.903(1)	$|F_o| > 4\sigma F$	648
V (Å^3)	442.58	R_1 (%)	1.92
Space group	$C2/c$	wR_2 (%)	5.68
Z	2	GooF	1.297
e$^-$(M1)	17.4(1)		
e$^-$(M2)	20.2(1)		
e$^-$M(1,2)	37.6(1)		
e$^-$M(1,2)^{EMPA}	37.8(2)		

$R_1 = \Sigma||F_o| - |F_c||/\Sigma|F_o|$
$wR_2 = \{\Sigma[w(F_o^2 - F_c^2)^2]/\Sigma[w(F_o^2)^2]\}^{\frac{1}{2}}$
GooF $= \{\Sigma [w(F_o^2 - F_c^2)^2]/(n-p)\}^{\frac{1}{2}}$, where n is the number of reflections and p is the total number of refined parameters.
$w = 1 / [\sigma^2(F_o^2) + (aP)^2 + bP]$, where P $= [Max(F_o^2,0) + 2 Fc^2]/3$

Table 2. Atom coordinates and isotropic-displacement parameters (Å^2) for D'Orbigny druse clinopyroxene.

	x	y	z	U_{eq}
T	0.28766(4)	0.09298(4)	0.2295(1)	0.0083(2)
M1	0	0.9073(1)	¼	0.0085(2)
M2	0	0.3018(2)	¼	0.0124(2)
M2′	0	0.2533(36)	¼	0.0124(2)
O1	0.1149(1)	0.0874(1)	0.1416(2)	0.0129(2)
O2	0.3625(1)	0.2520(1)	0.3218(2)	0.0151(2)
O3	0.3518(1)	0.0191(1)	−0.0060(2)	0.0129(2)

Table 3. Selected interatomic distances (Å) and angles (°) for D'Orbigny druse clinopyroxene.

T–O1	1.624(1)	M2–O1 × 2	2.365(2)
T–O2	1.608(1)	M2–O2 × 2	2.343(1)
T–O3	1.674(1)	M2–O3 × 2	2.570(2)
T–O3	1.692(1)	M2–O3 × 2	2.708(1)
<T–O>	1.650	<M2–O>	2.497
M1–O1 × 2	2.067(1)	M2′–O1 × 2	2.031(24)
M1–O1 × 2	2.126(1)	M2′–O2 × 2	2.294(1)
M1–O2 × 2	2.036(1)	M2′–O3 × 2	2.909(26)
<M1–O>	2.076	M2′–O3 × 2	2.983(22)
T–O3–T	135.8(1)		
O3–O3–O3	165.4(1)		

assigning the M1,2 site-populations. ^{VI}Al, Ti and Cr, taken from the unit formula (Table 4), were considered fully ordered at the M1 site, and we refine occupancies for Mg and Fe at M1, Ca at M2 and Fe at M2′. The refined occupancies at the M2 and M2′ sites are not reliable as the separation of the two sites is considerably less than the wavelength of the X-rays used in the diffraction experiment. However, the sum of the occupancies at M2 + M2′ is an accurate measure of the total scattering at the aggregate M2 + M2′ site. All Ca was assigned to M2 + M2′, leaving a deficiency of 0.056 pfu. All Mn was

Table 4. Average chemical composition (wt%) and unit formula (*apfu*) for D'Orbigny druse clinopyroxene.

SiO$_2$	45.84	Si	1.742
TiO$_2$	1.54	^{IV}Al	0.258
Al$_2$O$_3$	8.56	Σ	2.000
Cr$_2$O$_3$	0.34		
FeO	12.4	^{VI}Al	0.125
MnO	0.13	Ti	0.044
MgO	8.46	Cr	0.010
CaO	23.18	Fe^{3+}	0.035(1)
Total	100.45	Fe^{2+}	0.359(5)
		Mn	0.004
		Mg	0.479
		Ca	0.944
		Σ	2.000
		Fe^{3+}/Fe^{2+}	0.097

Table 5. Site-populations (*apfu*) for D'Orbigny druse clinopyroxene.

T	Si	1.742
	^{IV}Al	0.258
	Σ	2.000
M1	^{VI}Al	0.125
	Ti	0.044
	Cr	0.010
	Fe^{3+}	0.035
	Fe^{2+}	0.317
	Mg	0.469
	Σ	1.000
M2	Ca	0.944
	Mn	0.004
	Fe^{2+}	0.042
	Mg	0.010
	Σ	1.000
	R^{3+}	0.214
	KD	0.161

Note: R^{3+} = ^{VI}Al + Fe^{3+} + Ti + Cr.
K_D = Fe^{2+}(M1).Mg(M2)/Fe^{2+}(M2).Mg(M1).

assigned to M2 + M2′, and the balance of the site-scattering was assigned to Fe + Mg under the constraint that the sum of the occupancies at M2 + M2′ is 1.000 apfu. The resultant site populations (Table 5) reflect the refined total scattering at the aggregate M2 + M2′ site (20.2 *epfu*). All ^{VI}Al, ^{VI}Fe^{3+}, Cr^{3+} and Ti^{4+} were assigned to M1 on the basis of their known behavior in the pyroxene structure, and the balance of the Mg and Fe^{2+} was assigned to the M1 site; the calculated site-scattering (17.6 *epfu*) is in accord with the refined site-scattering (17.4 *epfu*) at M1.

Mössbauer Spectroscopy

Figure 1 shows the RT Mössbauer spectrum of D'Orbigny druse clinopyroxene, (a) single-crystal; (b) powder, and the corresponding Fe^{2+} QSD curve. It is composed of two strong absorption peaks at ~0.1 mm/s and ~2.2 mm/s resulting from
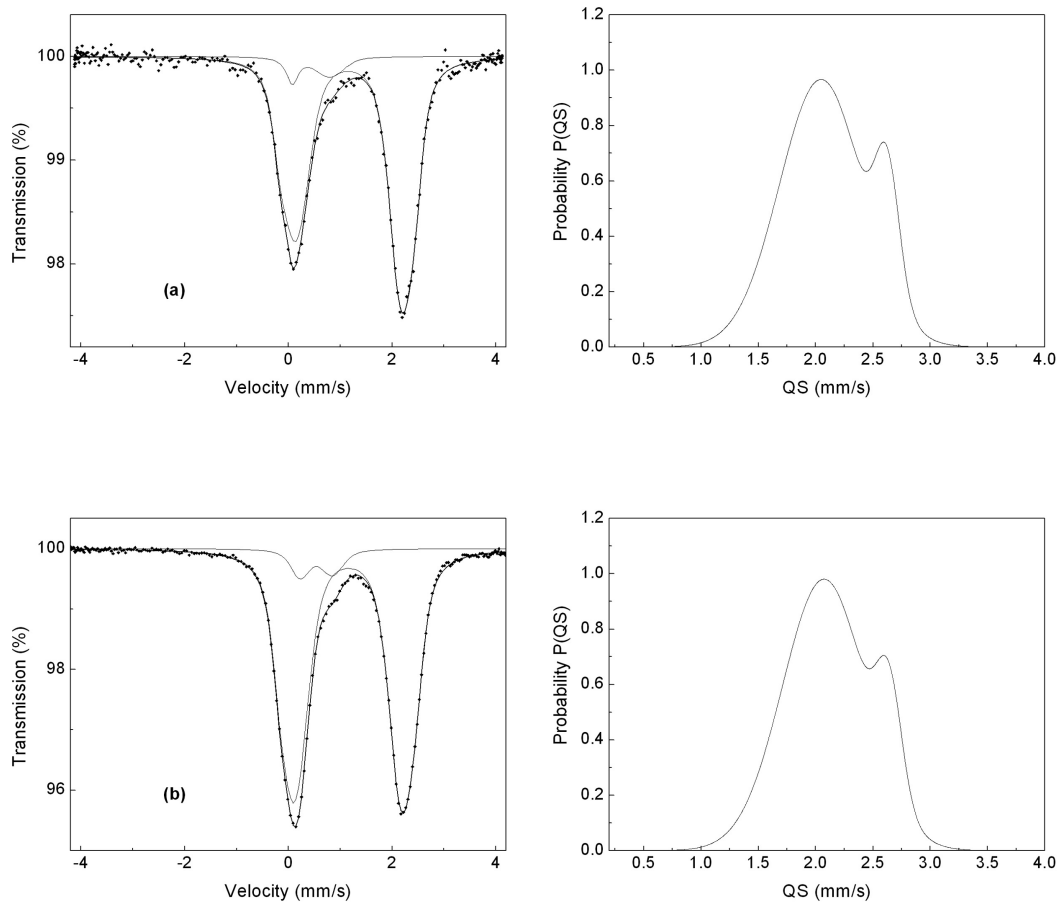
Fig. 1. Room-temperature Mössbauer spectrum of D'Orbigny druse clinopyroxene fitted with a Voigt-based quadrupole-splitting-distribution (QSD) method, (a) single-crystal, (b) powder, and the corresponding Fe^{2+} QSD curve. Solid subspectrum: Fe^{2+} site; dashed subspectrum: Fe^{3+} site.

the presence of Fe^{2+}, and a shoulder at ~0.9 mm/s representing the high-velocity peak of Fe^{3+}. The spectra were fit using a Voigt-based QSD analysis to a model having two generalized sites, one for Fe^{2+} with two Gaussian components and one for Fe^{3+} with one Gaussian component. The linewidth (Γ) of the symmetrical elemental doublets (asymmetrical doublets for the single-crystal spectrum) of the QSD was allowed to vary during the fitting procedure, and the centre shift (CS) is taken to be linearly correlated to the quadrupole splitting (QS) for both Fe^{2+} and Fe^{3+} sites. The resulting hyperfine parameters for the powder sample are given in Table 6.

The QSD curve for Fe^{2+} (Fig. 1) displays two Gaussian components centered at 2.07 mm/s and 2.64 mm/s, with 83% and 10% relative areas, respectively. The QS (2.07 mm/s) of the component with 83% relative area is very close to the QS values reported for Fe^{2+} at the M2 site in Ca-rich clinopyroxenes (~2.1 mm/s at RT) (Bancroft et al. 1971; De Grave and Eechhout 2003). However, the structure refinement and EMPA indicate that the amount of Fe^{2+} at the M2 site is 0.042 *apfu*, which is expected to give a relative area of 11%. Therefore, the Fe^{2+} QSD curve is mostly due to Fe^{2+} at the M1 site. Considering NNN effects, each M1 octahedron shares edges with three M2 polyhedra. Combining the very

small amounts of Mn and Mg with Fe^{2+} at M2 to Fe, we may recognize four different NNN configurations of M2 cations around the M1 site: (3Ca,0Fe), (2Ca,1Fe), (1Ca,2Fe), and (0Ca,3Fe). Assuming a random distribution of Ca and Fe, the probability of these configurations can be calculated using the binomial distribution (Dowty and Lindsley 1973). The probability of the M1(3Ca,0Fe) configuration is 0.84 and that of M1(2Ca,1Fe) is 0.15. The other two configurations have near-zero probabilities and can therefore be neglected. The predicted relative areas for Fe^{2+} at M1(3Ca,0Fe) and M1(2Ca,1Fe), calculated by normalizing and multiplying the above probabilities by the fraction of Fe^{2+} at M1, are 70% and 12%, respectively. Therefore, the Gaussian component with the larger QS (2.64 mm/s) can be assigned to Fe^{2+} at M1(2Ca,1Fe), and the component with the smaller QS (2.07 mm/s) is predominately due to Fe^{2+} at M1(3Ca,0Fe). The spectral contribution of Fe^{2+} at M2 (11% expected relative area) is strongly overlapping with that of Fe^{2+} at M1(3Ca,0Fe) and is very difficult to resolve. Table 6 summarizes the RT hyperfine parameters of the powdered sample of D'Orbigny druse clinopyroxene, along with the predicted relative areas for Fe^{2+}. The observed and predicted relative areas for Fe^{2+} are in very close agreement (Table 6).

Table 6. Room-temperature Mössbauer hyperfine parameters for D'Orbigny druse clinopyroxene powdered sample derived from a Voigt-based QSD fit.

Assignment	CS (mm/s)	QS (mm/s)	Γ (mm/s)	A (%) Measured	A (%) Calculated
Fe^{2+} [M1(2Ca,1Fe)]	1.15	2.64	0.28	10	12
Fe^{2+} [M1(3Ca,0Fe) + M2]	1.16	2.07		83	81
Fe^{3+} [M1]	0.54	0.62		7	–

Note: CS = center shift relative to α-Fe (±0.03 mm/s for Fe^{2+}, ±0.05 mm/s for Fe^{3+}); QS = quadrupole splitting (±0.04 mm/s for Fe^{2+}, ±0.07 mm/s for Fe^{3+}); A = relative area (±5% Fe^{2+}, ±2% for Fe^{3+}); Γ = linewidth of the elemental doublets of the QSD (±0.02 mm/s).

Redox and Thermal History of D'Orbigny

The amount of Fe^{3+} calculated from EMPA on the basis of charge balance is 0.035 *apfu* (Table 4). This value corresponds to a Fe^{3+}/Fe_{tot} ratio of 9(±3)%, in very good agreement with the value determined from Mössbauer spectroscopy, 7(±2)%, Table 6, for the powder sample. The RT spectrum of D'Orbigny druse clinopyroxene single-crystal gave a similar value of Fe^{3+}/Fe_{tot} (7%). Therefore, it seems that Fe^{3+} is structural and we assign it to the M1 site.

The presence of Fe^{3+} in D'Orbigny druse clinopyroxene may indicate the crystallization of this phase under oxidizing conditions, in accord with the suggestion of Kurat et al. (2004) that redox conditions were oxidizing during the formation of D'Orbigny clinopyroxenes. The results are also consistent with the melting experiments of chondrites, where melting under relatively high oxygen fugacity produced melts that are similar to angrites while melting under reducing conditions resulted in melts similar to eucrites (Jurewicz et al. 1993).

Applying the oxygen barometer of Cortés et al. (2006), the oxygen fugacity with reference to the quartz-fayalite-magnetite (QFM) buffer can be estimated using the Fe^{3+}/Fe^{2+} ratio in clinopyroxene as follows:

$$\Delta QFM = -1.801(Fe^{3+}/Fe^{2+})^2 + 8.753(Fe^{3+}/Fe^{2+}) - 0.943$$

Substituting the Fe^{3+}/Fe^{2+} value for D'Orbigny druse clinopyroxene (Table 4), we obtain $\Delta QFM \approx 0$. This indicates that D'Orbigny druse clinopyroxes may have crystallized at redox conditions very close to the QFM buffer, the conditions at which most of the terrestrial rocks in the lower crust have been formed.

To estimate the closure temperature of the intracrystalline Fe^{2+}-Mg exchange reaction in D'Orbigny druse clinopyroxene, we use the geothermometric equation of Brizi et al. (2000), where the effect of composition on the geothermometric calibration is taken into account:

$$T(K) = [12100 - 27700 (Ca+Na+R^{3+}) + 20400 (Ca+Na+R^{3+})^2]/$$
$$[-lnK_D + 7.1 - 20.3 (Ca+Na+R^{3+}) + 15.2 (Ca+Na+R^{3+})^2]$$

where $R^{3+} = {}^{VI}Al + Fe^{3+} + Ti + Cr$. The resulting closure temperature is 1000 °C. This temperature is consistent with the heating experiments on $En_{46}Fs_{11}Wo_{43}$ augite, where an equilibrium K_D value of 0.151 was obtained when the augite sample was annealed at 950 °C (Brizi et al. 2001). It is also in agreement with the postulated scenario that the minerals coexisting in D'Orbigny record successive events, the latest event being highly oxidizing and taking place at ~1000 °C (Kurat et al. 2004).

Mao et al. (1977) reported a Mössbauer study of a clinopyroxene (fassaite) from the Angra dos Reis (ADOR) meteorite. The room temperature Mössbauer spectrum of ADOR clinopyroxene (Mao et al. 1977) shows an asymmetric doublet and was fitted with two superimposed Lorentzian doublets due to Fe^{2+} in M1 and M2 sites, although the crystal structure refinement (Hazen and Finger 1977) indicates that the M2 site is almost fully occupied by Ca (0.97 apfu), and no Fe^{3+} was detected. However, the quality of the spectrum and the adopted fitting procedure could have contributed to obscure a small possible Fe^{3+} contribution. Nevertheless, Hazen and Finger (1977), using the structure refinement data, obtained a closure temperature of 1100 °C for ADOR clinopyroxene, similar to the closure temperature of the druse clinopyroxenes of D'Orbigny.

Genetic Implications of Our Results

The genesis of angrites is a subject of ongoing debates. The most widely accepted model sees them as igneous rocks of basaltic composition originating from a differentiated planetesimal (e.g., Treiman 1989; Mittlefehldt and Lindstrom 1990; Longhi 1999; Mittlefehldt et al. 2002). However, this model faces several conflicts with mineralogical and chemical observations (e.g., Prinz et al. 1977, 1988; McKay et al. 1988; Treiman 1989; Jurewicz et al. 1993; Mittlefehldt et al. 2002). Because all phases are commonly out of equilibrium with each other (Prinz and Weisberg 1995; Kurat et al. 2004), the mineralogical and bulk chemical properties of angrites remain peculiar.

Recent studies performed on the dense part of D'Orbigny suggest that this rock formed from a melt by rapid and complete crystallization (Mittlefehldt et al. 2001, 2002). However, mineralogical and chemical studies of the dense and the coarse-grained porous part, which contains abundant open druses, led Kurat et al. (2004) and Varela et al. (2003, 2005) to challenge this igneous model, postulating that D'Orbigny could have formed in the solar nebula under

changing redox conditions. The location of the sizable, euhedral pyroxene crystals in open spaces—druses—already indicates that they did not grow from a silicate melt but very possibly are the result of a pneumatolytic process. In addition, the trace element contents of the late aluminous hedenbergite show features (e.g., underabundance of Sc) that are incompatible with formation from the bulk system's residual melt (Varela et al. 2005).

This study cannot be expected to solve that problem but can provide some facts that can bring us closer to an answer. It was undertaken to create a state-of-the-art crystallographic analysis of an unusual pyroxene. It was also undertaken to quantify some of the parameters related with the last thermal history of this rock, as follows:

1. Druse pyroxenes were formed under redox conditions very close to the QFM buffer.
2. They were cooled quickly as documented by the preservation of the high-temperature cation distribution in the pyroxene structure.
3. This indicates a closure temperature of $\approx$1000 °C.

These results, however, pose another contradiction as on one side, the high closure temperature obtained for D'Orbigny druse clinopyroxene indicates an extremely fast cooling rate (Molin and Zanazzi 1991), but, on the other hand, the chemical homogeneity of these druse clinopyroxenes suggests a slow cooling (McKay et al. 1993).

The last quick cooling event—with a closure temperature of $\approx$1000 °C—seems to put some constraints to the last high-temperature thermal episode (e.g., addition of more primitive melts) invoked to explain the zoning in olivine-subcalcic kirschsteinites and clinopyroxenes of D'Orbigny (Mittlefehldt et al. 2002). If the druse pyroxenes were in contact with a gas phase (e.g., pneumatolytic event in a carrier body or in the nebula), the quick cooling of the crystals could have been caused by dissipation of the hot vapor.

Editorial Handling—Dr. Allan Treiman

REFERENCES

Brizi E., Molin G., and Zanazzi P. F. 2000. Experimental study of intracrystalline Fe^{2+}-Mg exchange in three augite crystals: Effect of composition on geothermometric calibration. *American Mineralogist* 85:1375–1382.

Brizi E., Molin G., Zanazzi P. F., and Merli M. 2001. Ordering kinetics of Mg-Fe^{2+} exchange in a $Wo_{43}En_{46}Fs_{11}$ augite. *American Mineralogist* 86:271–278.

Bruno E., Carbonin S., and Molin G. 1982. Crystal structure of Ca-rich clinopyroxenes on the $CaMgSi_2O_6$–$Mg_2Si_2O_6$ join. *TMPM Tschermaks Mineralogische und Petrographische Mitteilungen* 29:223–240.

Cameron M. and Papike J. J. 1980. Crystal chemistry of silicate pyroxenes. In *Pyroxenes*, edited by Prewitt C. T. Reviews in Mineralogy, vol. 7. Washington, D. C.: Mineralogical Society of America. pp. 1–92.

Cortés J. A., Wilson M., Condliffe E., and Francalanci L. 2006. The occurrence of forsterite and highly oxidizing conditions in basaltic lavas from Stromboli volcano, Italy. *Journal of Petrology* 47:1345–1373.

De Grave E. and Eechhout S. G. 2003. ^{57}Fe Mössbauer-effect studies of Ca-rich, Fe-bearing clinopyroxenes: Part III. Diopside. *American Mineralogist* 88:1145–1152.

Dowty E. and Lindsley D. H. 1973. Mössbauer spectra of synthetic hedenbergite-ferrosilite pyroxenes. *American Mineralogist* 58: 850–868.

Dundon R. W. and Hafner S. S. 1971. Cation disorder in shocked orthopyroxenes. *Science* 174:581–583.

Floss C., Crozaz G., McKay G., Mikouchi T., and Killgore M. 2003. Petrogenesis of angrites. *Geochimica et Cosmochimica Acta* 67: 4775–4789.

Hazen R. M. and Finger L. W. 1977. Crystal structure and compositional variation of Angra dos Reis fassaite. *Earth and Planetary Science Letters* 35:357–362.

Ibers J. A. and Hamilton W. C. 1992. *International tables for X-ray crystallography IV.* Birmingham, U.K.: Kynoch Press.

Jurewicz A. J. G., Mittlefehldt D. W., and Jones J. H. 1993. Experimental partial melting of the Allende (CV) and Murchison (CM) chondrites and the origin of asteroidal basalts. *Geochimica et Cosmochimica Acta* 57:2123–2139.

Kurat G., Varela M. E., Brandstätter F., Weckwerth G., Clayton R. N., Weber H. W., Schultz L., Wäsch E., and Nazarov M. A. 2004. D'Orbigny: A non-igneous angritic achondrite? *Geochimica et Cosmochimica Acta* 68:1901–1921.

Longhi J. 1999. Phase equilibrium constraints on angrite petrogenesis. *Geochimica et Cosmochimica Acta* 63:573–585.

Malgarotto C., Molin G., and Zanazzi P. F. 1993. Cooling history of a dyke on Alicudi (Aeolian Islands) from intracrystalline Fe^{2+}-Mg exchange reaction in clinopyroxene. *European Journal of Mineralogy* 5:755–762.

Mao H. K., Bell P. M., and Virgo D. 1977. Crystal-field spectra of fassaite from the Angra dos Reis meteorite. *Earth and Planetary Science Letters* 35:352–356.

McCallister R. H., Finger L. W., and Ohashi Y. 1976. Intracrystalline Fe^{2+}-Mg equilibria in three natural Ca-rich clinopyroxenes. *American Mineralogist* 61:671–676.

McKay G., Lindstrom D., Le L., and Yang S. R. 1988. Experimental studies on synthetic LEW 86010 analogs: Petrogenesis of a unique achondrite (abstract). 19th Lunar and Planetary Science Conference. pp. 760–761.

McKay G., Ogawa T., Miyamoto M., and Takeda H. 1993. More on the cooling history of angrite LEW 86010. 24th Lunar and Planetary Science Conference. pp. 967–968.

Mittlefehldt D. W. and Lindstrom M. M. 1990. Geochemistry and genesis of angrites. *Geochimica et Cosmochimica Acta* 54:3209–3218.

Mittlefehldt D. W., Killgore M., and Lee M. T. 2001. Petrology and geochemistry of the new angrite D'Orbigny (abstract #2057). 32nd Lunar and Planetary Science Conference. CD-ROM.

Mittlefehldt D., Killgore M., and Lee M. T. 2002. Petrology and geochemistry of D'Orbigny, geochemistry of Sahara 99555, and the origin of angrites. *Meteoritics & Planetary Science* 37:345–369.

Molin G. and Zanazzi P. F. 1991. Intracrystalline Fe^{2+}-Mg ordering in augite: Experimental study and geothermometric applications. *European Journal of Mineralogy* 3:863–875.

Morimoto N. 1989. Nomenclature of pyroxenes. *Canadian Mineralogist* 27:143–156.

Prinz M., Keil K., Hlava P. F., Berkley J. L., Gomes C. B., and Curvello W. S. 1977. Studies of Brazilian meteorites III. Origin and history of the Angra dos Reis achondrite. *Earth and Planetary Science Letters* 35:317–330.

Prinz M., Weisberg M. K., and Nehru C. E. 1988. LEW 86010, a second angrite: Relationship to CAIs and opaque matrix (abstract). 19th Lunar and Planetary Science Conference. pp. 949–950.

Prinz M. and Weisberg M. K. 1995. Asuka 881371 and the angrites: Origin in a heterogeneous, CAI-enriched, differentiated, volatile-depleted body (abstract). 20th Symposium on Antarctic Meteorites. pp. 207–210.

Rancourt D. G. and Ping J. Y. 1991. Voigt-based methods for arbitrary-shape static hyperfine parameter distributions in Mössbauer spectroscopy. *Nuclear Instruments and Methods in Physics Research B* 58:85–97.

Sheldrick G. M. 1997. SHELX97 program for the solution and refinement of crystal structures. University of Göttingen, Germany.

Skogby H., Annersten H., Domeneghetti M. C., Molin G. M., and Tazzoli V. 1992. Iron distribution in orthopyroxene: A comparison of Mössbauer spectroscopy and X-ray refinement results. *European Journal of Mineralogy* 4:441–452.

Treiman A. H. 1989. An alternate hypothesis for the origin of Angra dos Reis: Porphyry, not cumulate. Proceedings, 19th Lunar and Planetary Science Conference. pp. 443–450.

Varela M. E., Kurat G., Zinner E., Métrich N., Brandstätter F., Ntaflos T., and Sylvester P. J. 2003. Glasses in the D'Orbigny angrite. *Geochimica et Cosmochimica Acta* 67:5027–5046.

Varela M. E., Kurat G., Zinner E., Zinner E., Hoppe P., Ntaflos T., and Nazarov M. A. 2005. The non-igneous genesis of angrites: Support from trace element distribution between phases in D'Orbigny. *Meteoritics & Planetary Science* 40:1–22.

Williams P. G. L., Bancroft G. M., Brown M. G., and Turnock A. C. 1971. Anomalous Mössbauer spectra of C2/c clinopyroxenes. *Nature (Physical Science)* 230:149–151.

APPENDIX: EXPRESSION OF D'ORBIGNY PYROXENE IN TERMS OF END-MEMBER COMPONENTS

The compositions for druse pyroxene and core and rim groundmass pyroxene are given in Table A1; for the core and rim groundmass-pyroxene compositions, the Fe^{3+} content was calculated from the chemical analyses in the usual manner, and cations were likewise assigned to the various sites. End-member compositions encompassing the D'Orbigny pyroxenes are listed in Table A1. CATS accommodates some tetrahedrally and octahedrally coordinated Al ($+ Fe^{3+} + Cr^{3+}$), and TICATS accommodates some tetrahedrally coordinated Al and octahedrally coordinated Ti. Note that we consider the formulation $R^{2+} R^{2+}_{0.5}R^{4+}_{0.5} R^{3+}R^{4+} O_6$ (Morimoto 1989) completely unsuitable as a component for the following reasons: 1) it is not irreducible, as it may be factored into the components $R^{2+} R^{2+} R^{4+}_2 O_6$ and $R^{2+} R^{4+} R^{3+}_2 O_6$; 2) there is no way of rigorously distinguishing between the components Ca MgTi AlSi O_6 and Ca Fe^{2+}Ti AlSi O_6. For the rim composition of the groundmass pyroxene, $(Si + Al + Fe^{3+} + Cr^{3+})$ <2 apfu (atoms per formula unit), and requires assignment of Ti^{4+} or vacancy to the T site. As there is no confirmed occurrence of Ti^{4+} or vacancy at the T site in pyroxene, this is presumably an error. In order to calculate the components for this particular pyroxene, we introduce the component TIHD, Ca Fe^* Ti^{4+}Si O_6, recognizing that it represents error in the analysis, albeit small (Table A1). We have calculated the components in the EN-FS-WO plane in two ways: 1) as structural pyroxene components EN-FS-DI-HD and 2) as chemical components EN-FS-WO (Table A1); the compositions of the pyroxenes may be expressed in either form.

Table A1. D'Orbigny pyroxenes expressed in terms of various end members.

	End member	Druse cpx	Groundmass cpx[*]	
			Core	Rim
TICATS	$CaTi^{4+}Al^*_2O_6$	0.044	0.034	0.127
TIHD	$CaFe^*Ti^{4+}SiO_6$	0	0	0.015
CATS	$CaAl^*AlSiO_6$	0.170	0.142	0
DI	$CaMgSi_2O_6$	0.479	0.494	0.004
HD	$CaFe^*Si_2O_6$	0.251	0.267	0.832
EN	$MgMgSi_2O_6$	0	0	0
FS	$Fe^*Fe^*Si_2O_6$	0.056	0.063	0.022
Sum		1.000	1.000	1.000
WO	$Ca_2Si_2O_6$	0.365	0.380	0.418
EN	$MgMgSi_2O_6$	0.240	0.247	0.002
FS	$Fe^*Fe^*Si_2O_6$	0.181	0.197	0.438

Note: $Fe^* = Fe^{2+} + Mn^{2+}$; $Al^* = Al + Fe^{3+} + Cr^{3+}$.
[*]Core and rim groundmass clinopyroxene compositions were calculated from the microprobe data of Kurat et al. (2004).